Fuel 224 (2018) 529–536

Contents lists available at ScienceDirect

Fuel

journal homepage: www.elsevier.com/locate/fuel

Full Length Article

A comprehensive investigation of refinery preheaters foulant samples originated by heavy crude oil fractions as heating fluids

Elaheh Behranvand[a], Mohammad Reza Mozdianfard[a,*], Emilio Diaz-Bejarano[b], Francesco Coletti[c,d], Pawel Orzlowski[b], Sandro Macchietto[b,c]

[a] Chem. Eng. Dep., Eng. Faculty, University of Kashan, Kashan, Iran
[b] Dept. of Chem. Eng., Imperial College London, London SW7 2AZ, UK
[c] Hexxcell Ltd., Innovation Hub, White City Campus, 80 Wood Lane, London W12 0BZ, UK
[d] College of Engineering, Design and Physical Sciences, Brunel University London, Uxbridge, UB8 3PH, UK

ARTICLE INFO

Keywords:
Refinery foulant characterization
Fouling mechanism
Corrosion
Vacuum gas oil
Vacuum bottom
Iron oxide

ABSTRACT

A deep understanding of the mechanisms responsible for fouling from both crude oils and their fractions is paramount to ensure efficient energy recovery in heat exchangers of crude preheat trains. In this work, seven samples of fouling deposits, carefully collected from a number of refinery heat exchangers processing vacuum gas oil (VGO) and vacuum bottom (VB) streams in an atmospheric crude preheat train were investigated using a range of characterization techniques with the aim of identifying the underlying mechanisms that led to deposition. Characterization of the deposits included morphological and physical examination, fractionating solubility test, Scanning Electron Microscopy-Energy Dispersive X-ray, Combustion Analysis and X-ray Diffraction. In all samples examined, more than 75 wt% of the deposits were identified as inorganic, with about 50 wt% being FeS. At 270–300 °C, FeO(OH) was also identified to be deposited on the tube surfaces made in Cr steel alloy, where more fouling and less corrosion were evident compared to carbon steel (CS). These observations were found in agreement with recent laboratory studies aimed at identifying the role of temperature and tube material in petroleum corrosion. Furthermore, sulphur crystals were found in several VGO fouling samples. Based on the experimental results obtained, a mechanism was proposed to explain the corrosion fouling phenomenon, considered to be the underlying mechanism affecting the refinery. The mechanism involves naphthenic acid attack to the tubes' metal surface, decomposition of iron naphthenate, disproportion of iron oxide and sulphidation reactions. The results highlighted the importance of studying deposits formed under industrial conditions, timescales and variation of the deposition process, evidenced by the deposit characteristics, along extensive heat exchanger networks.

1. Introduction

Atmospheric crude distillation is the first process unit in oil refineries. The performance of the distillation columns where oil is fractionated into products affects significantly that of the entire crude oil refining process. The most important factor influencing the column performance is the crude oil inlet temperature, together with the flowrates and temperatures of the recycled fluids. A significant portion of the thermal energy in product streams leaving the distillation column is recovered by a network of heat exchangers, the pre-heat train, in which the inlet crude oil is heated up before entering the furnace. The study of fouling in these exchangers has been the subject of intense interest from both academia and industry and its impact on operations, energy costs and environmental emissions has been well documented [1,2], however the underlying phenomena are still largely poorly understood.

Many fouling mechanisms have been identified to occur in crude pre-heat trains [3]. These include scaling (salt precipitation), corrosion, precipitation (by cooling, blending or breaking of emulsions), chemical reaction (thermal cracking, polymerisation of conjugated olefins, aromatic growth, oxidation, etc.), and particulate deposition (such as entrained coke, asphaltenes, iron sulphides) which could act individually or in combination with each other. Characterization of fouling deposits is an important first step in understanding the underlying mechanisms. For instance, when 10–15 wt% or more inorganic components are detected in a fouling sample, this could be a good indication that either scaling, corrosion and particulate are the possible mechanisms responsible for deposition [4,5].

* Corresponding author.
E-mail address: mozdianfard@kashanu.ac.ir (M.R. Mozdianfard).

https://doi.org/10.1016/j.fuel.2018.03.077
Received 14 July 2017; Received in revised form 8 March 2018; Accepted 13 March 2018
Available online 30 March 2018

Table 1
The operational information of foulant samples.

Samples	VGTO-1	VGTO-2	VGTO-3	VGTO-4	VGTO-5	VBTI-1	VBTO-2
Origin Fluid	VGO	VGO	VGO	VGO	VGO	VB	VB
Exchanger Name	E1A	E2B	E2A	E3B	E3A	E4	E5
Tube Material	C.S.	C.S.		1¼ Cr-1/2 Mo		C.S.	5Cr-1/2Mo
Max Bulk Temp Range (°C)	180–120	254–200		300–230		230–190	280–250

Several efforts are found in the literature attempting to standardise the generation, collection and analysis of crude oil samples. One such effort is the analytical industrial protocol patented by Brons et al. in 2004 [4]. The protocol details characterization methods for solids collected in refinery heat exchangers, that can be used to identify the mechanism/s involved in their generation. The analysis prescribed included methylene chloride or toluene extraction, Scanning Electron Microscopy-Energy Dispersive X-ray (SEM-EDX), Thermogravimetric Analysis (TGA), Elemental Analysis (EA) and Optical Microscopy (OM) arranged as a sequential diagram. In 2006, an industrial task force published recommended guidelines aimed at facilitating direct comparison between non-proprietary fouling data [5]. Techniques included were Fourier transform infrared spectroscopy (FTIR), X-ray fluorescence (XRF), X-ray diffraction (XRD), X-ray photoelectron spectroscopy and Nuclear magnetic resonance (NMR). In 2009, Venditti et al. [6] applied some of these techniques following solubility tests, size exclusion chromatography and UV-fluorescence to characterize four foulants deposited in a refinery heat exchanger by desalted crude oil, kerosene, vacuum gas oil and crude oil residue. In another work, Young et al. [7] employed the same analysis on deposits generated in a laboratory batch stirred cell. These deposits were then characterised and their thermal data were correlated with oil and deposits taken from various process conditions by measuring deposit thickness along and around the probe using a laser and coherent light scanning procedure. Recently, Joshi in [8], announced that the same simplified analysis proposed by Brons et al. [4] is sufficient for quantification of only a few elements, required to distinguish between the most common mechanisms of crude oil fouling. He also described the concept of setting a mass balance between the measured weight percentages of the identified elements to verify the quality of the results or to specify the necessity of more analysis to recognise the possible missing elements.

Analysis of deposits formed in lab-tests may help improve the fundamental understanding of the processed involved in fouling deposit formation. However, the conditions leading to deposition in industrial systems are very difficult to reproduce in lab-test, as a result of the complexity of crude oil composition, the frequent variation of feedstock and the long times scales for significant fouling build-up (months or years). Obtaining reliable outcomes requires appropriately collecting fouling samples from the heat exchangers in a refinery, while considering systematically their fluid properties and operating conditions. Foulant samples deposited by hydrocarbon fluids are complex materials containing both organics and inorganics. Their low solubility makes them unsuitable for characterization by common analytical techniques [6], and adequate protocols for sample preparation are required prior to the chemical characterization.

Following an uninterrupted 8-year field study on fouling of crude oil preheaters at a refinery in Iran processing the same feedstock [9,10], in this paper, several foulant samples deposited by vacuum gas oil and vacuum bottoms as heating fluids of crude oil were investigated. This was done by recording their general appearance, then carrying out a fractionating solubility test, SEM-EDX, XRD and combustion/CHN analysis. First, sample description, preparation and analysis in the experimental work are described, with results elucidated in three categories of morphology, physical and chemical characteristics. The presence of FeS and FeO(OH) is then discussed, taking into account laboratory case studies and the role of temperature and tube material. A novel corrosion/deposition mechanism is proposed to explain the observed results. Finally, the presence of sulphur crystals in the maltenes fractions of some vacuum gas oil (VGO) foulant samples is noted and suggested for further investigations.

2. Experimental

2.1. Samples

Foulant samples were collected during a major shutdown of a crude oil distillation unit following a 4-year period of operation. The collection was performed following water circulation and steam purging, after which the tube bundles were pulled out of their shells. Five samples were taken from foulant deposited by VGO and two from VB as heating fluids (see Table 1). The foulant originated by VGO presented greater volume compared to those of the other heating fluids, included that formed by VB.

In the refining process, VGO (of Specific Gravity SG = 0.9137) leaves the middle of the vacuum distillation column at about 300 °C. It is then cooled in the crude oil preheaters and air coolers and partly recycled back to the column, with the remainder sent to a hydrocracking unit for conversion into more valuable products. VB (SG = 1.0115), the heaviest material in the distillation columns, is pumped out from the bottom of the vacuum column at about 360 °C to the hot-end preheat exchangers.

Operational information of samples including the fluids from which foulants were originated, the exchangers name, tube material and maximum bulk temperature ranges (input-output) are listed in Table 1. As for the notation used in describing the foulant samples, VG and VB indicate the corresponding fluid, while TO and TI indicate whether the sample was taken from tube outer or inner surface, respectively. The higher the number at the end of the sample names, the higher was the operating temperature for that fluid.

2.2. Preparation

The analysis preparation step consisted in removing the free bulk fluid trapped in the foulant contents and converting it into powder for further analysis in the available equipment. Sufficient quantity (in 10 to 1 ratio) of n-heptane was added to10-25 g of sample in an airtight jar and kept for at least 4 h at room temperature. Using a vacuum pump, the mixture was filtered repeatedly using additional solvent until a colourless filtrate was obtained. This way, it was safe enough to assume that all trapped fluid was removed. The leftover on the filter paper was dried for at least 12 h in an oven at 60–80 °C, grinded with 60 mesh (250 μm) sieves, and mixed thoroughly [8,11].

2.3. Analysis

With a view to maintaining a simple strategy to characterize foulant samples and explore the prevailing mechanism/s, a set of analytical tests was carried out on the raw samples and powders prepared as explained above.

The general appearance of the raw samples was first recorded using a digital camera. The sample layer thickness was also measured when possible using a digital calliper with an accuracy of ± 0.01 mm.

A solvent extraction method, used elsewhere for product characterization in hydrocracking studies [12,13], was employed to fractionate the raw samples into three groups: maltenes (heptane soluble), asphaltenes (heptane insoluble, toluene soluble) and the remaining insoluble portion. To this purpose, a 0.2–0.5 g sample was placed in a jar (labelled as insoluble part) and mixed with 8.0 mL of heptane for 2 h, before centrifugation at 2000 rpm for 20 min. The supernatant was then separated and injected into the maltenes jar, while heptane was added to the rest of the sample to repeat the procedure at least three times, or until the supernatant became clear. Subsequently, toluene was added to the solids and mixed for 2 h and centrifuged, in order to extract the top phase which was transferred to the asphaltenes jar. Finally, three jars containing heptane soluble, toluene soluble and the insolubles were dried until constant weights were obtained by exposing them to a slight flow of Nitrogen. The jars weight changes were recorded accordingly. It should be noted that the insoluble fraction might contain inorganics and coke, in principle, the only organic compound insoluble in toluene [4].

The free trapped fluid foulants prepared in the form of powder were analysed by SEM-EDX, XRD and combustion analysis (CHN). For this study, a JEOL JSM-6010LA model SEM equipped with an Oxford INCA EDXS system was employed at an accelerating voltage of 20 kV, and a working distance ranging from 15 to 20 mm to detect SE and X-rays emissions. Samples were nonconductive dried powder with particle size larger than 1 μm, hence the analysis were carried out at high vacuum. The samples were mounted on a carbon tape which was stuck on a specimen stub. Excess particles were blown off with compressed air to remove piled particles, and coated with an ultrathin layer of gold. As for XRD analysis, foulant diffraction patterns were determined by an X'Pert Pro diffractometer (from PAN analytical) while mineral compositions were identified using PANalytical X'Pert HighScore Plus. To determine the weight percentage of C, H and N contents, 2 mg of the prepared samples was provided to a CHN analyser (Medac Ltd., UK) for the combustion analysis.

3. Results and discussion

3.1. Morphology and physical characteristics

Fig. 1 illustrates the general appearance of samples in images taken with a digital camera. The fouled layers deposited by VGO covered peripherally all-over the exchangers' tubes length, except for VGTO-1. The latter sample was collected from the tubes of the coolest exchanger (E1A). Its fouling deposit presented significantly less volume and exhibited particulates in nature, as shown in Fig. 1, VGTO-1(b). The foulant thickness, indicated beneath the corresponding images, became thinner as the operating temperatures decreased. Interestingly, samples deposited in the exchangers with the same mechanical design specifications (i.e., E3A and E3B, E2A and E2B, see Table 1) had similar appearance. However, those formed at the hotter shells of A (i.e., VGTO-5 and VGTO-3), were thicker (by 28% and 44%, respectively) and more brittle when collected. VB foulants deposited both inside (VBTI-1) and outside (VBTO-2) the exchangers' tubes had a metallic lustre appearance, with the former being like black particulates and the latter exhibiting a brighter flaky look.

The microscopic topography of foulant particles was examined by SEM images taken at 500 μm resolution and is presented in Fig. 2. Irregularly shaped particles in various quantity and sizes are observed, ranging from mostly fine aggregates to large agglomerated ones. Particles in VB foulant samples appeared more like polyhedral clusters with sharp edges.

The number of large agglomerated particles was quantified using a Digimizer software. First, the surface area of particles larger than a specific base size (here assumed 0.02 mm^2, as indicated in Fig. 3) was calculated. The number of particles was then counted and the results were illustrated graphically, together with an average surface areas value for all large particles in the sample (Fig. 4). Apart from VGTO-1, a sample which consisted mostly of fine aggregates, the number of large particles as well as the average surface area seems to be greater for the VB foulant samples. In VGO samples, both quantities were higher for foulants deposited in the hotter exchanger shells having the same design specifications. As explained below, the deposits formed in the hotter shells were thicker and more brittle. Therefore, the results seem to indicate that these properties are related to the number of large particles.

3.2. Chemical characteristics

The three fractions obtained after solvent extraction of the raw foulant samples are detailed in Table 2 in terms of wt% of maltenes, asphaltenes and insoluble parts. It is worth noting that VGO is an asphaltenes-free fraction of crude oil; very small increases in the asphaltenes jars weights observed for several samples were considered as analysis error and were therefore adjusted by adding them to the insoluble fraction. Amongst the VGO foulant samples examined (see Table 2), those deposited at higher temperatures contained less maltenes, and greater insoluble contents, similar to the VB's foulants which contained nearly 3% asphaltenes. Given the high content of inorganics in all samples tested, scaling, corrosion and particulate deposition were considered the most likely dominant fouling mechanisms.

Results of the EDX, CHN and XRD analysis on the free trapped fluid samples are summarized in Table 3. EDX determined the relative weight percentage of most elements in the samples except for carbon and hydrogen which were specified by combustion analysis in absolute terms. Hence, the relative EDX results were normalized in order to provide an appropriate comparable data, according to Joshi's approach, which involves setting up a mass balance between the obtained data [8]. As can be seen from Table 3, for nearly all samples taken from the VGO and VB heating fluids, the content of C, H, N, O, S and Fe was significant (higher than ~1.0 wt%), and composed partly by FeS, FeO(OH) and S in crystalline forms as indicated by their peaks indexed on the XRD patterns of Fig. 5. Interestingly, peaks associated with FeS were clearly repeated in all of the patterns, while FeO(OH) peaks seem to exist only in VGTO-5, VGTO-4 and VBTI-2, with S peaks being observed just in the first two. The relatively small percentage of C indicates that the organic material in the raw deposit samples was most likely trapped, non-coked oil; therefore material soluble in heptane and washed away from samples during the preparation step.

It should be mentioned that Na content in the VB samples was noticeable (0.87 wt% and 2.07 wt%) compared to that in VGO samples (0.00–0.23 wt%). However, fouling concerns caused by VB as heating fluid were insignificant compared to those of VGO and as such, the role of Na was not considered in the discussion that follows.

3.3. Fouling mechanism determination

The evidence relating to tube materials, operating temperatures of exchangers, foulant layers thickness, insoluble fraction, elements and compounds identified (see Fig. 1 and Tables 1–3) point to the followings remarks:

a. More than 75 wt% of each free trapped fluid sample were inorganic matter, mostly (> 50%) in the form of Fe and S elements, which were deposited at temperatures lower than 300 °C. Based on XRD evidence, Iron sulphide (FeS) existed in all of them.
b. Foulant layers were thicker in the first two VGO samples deposited at higher operating temperatures on Cr-Mo alloy tubes (1.25 and 0.98 mm for VGTO-5 and 4) compared to those formed on the outer surfaces of CS tubes at lower operating temperatures (0.56 and 0.39 mm for VGTO-3 and 2), while the former had less Fe and S content.
c. FeO(OH) existed only in samples deposited at higher temperatures

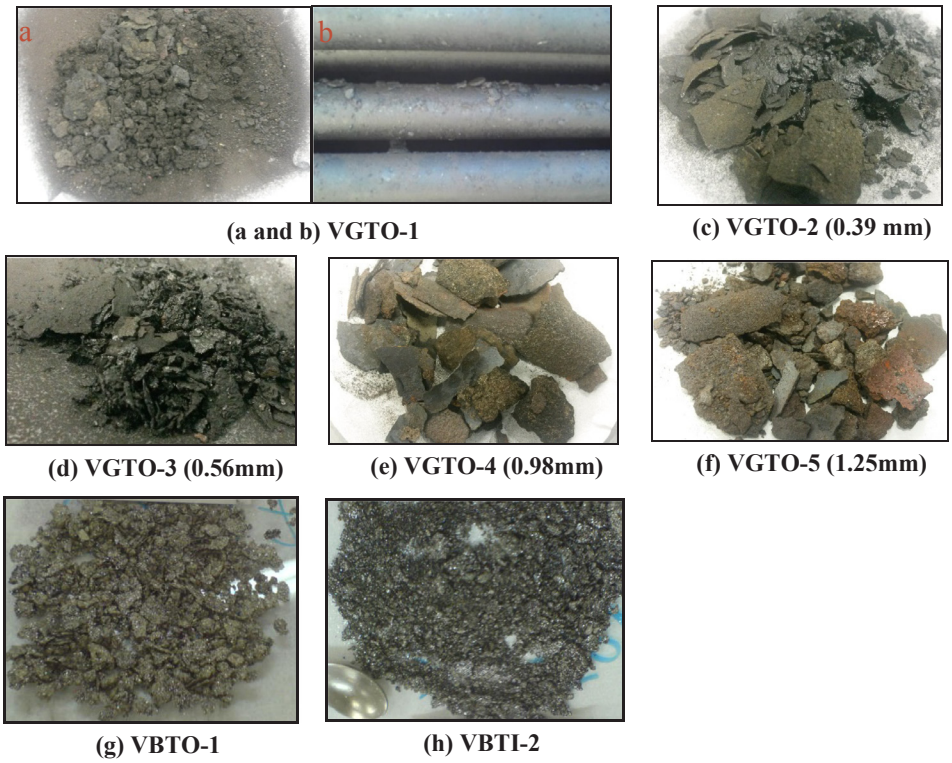

Fig. 1. General appearance of raw foulant samples (foulant layer thickness given in mm where possible).

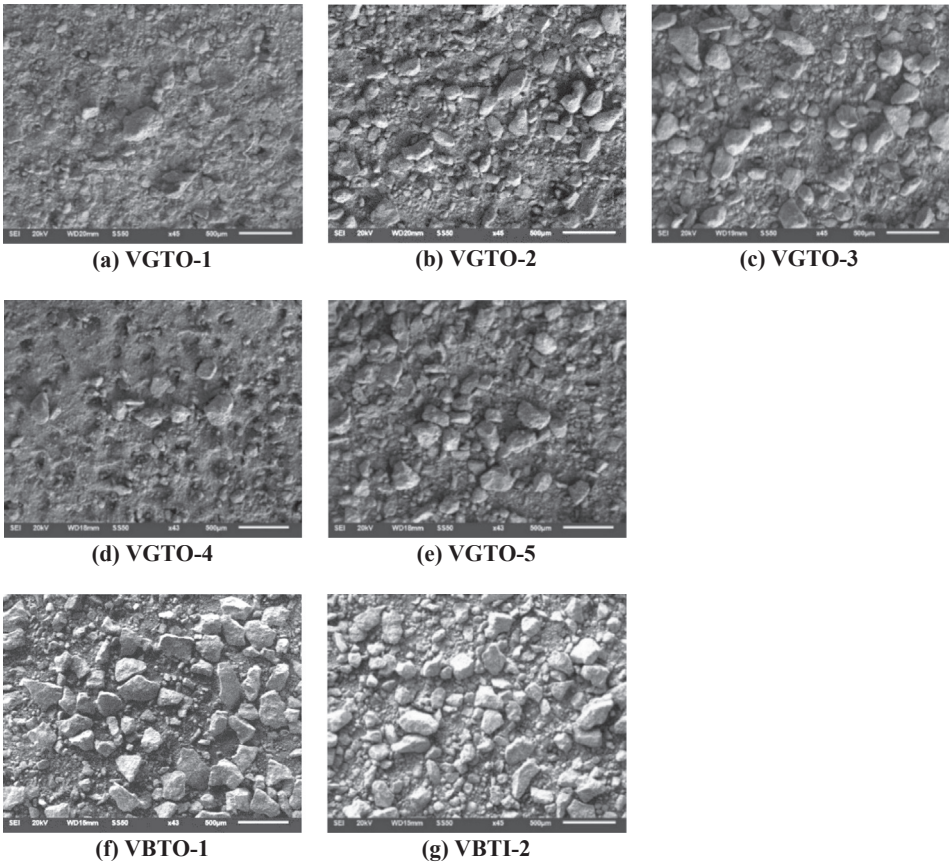

Fig. 2. SEM images of foulant samples taken at a 500 μm resolution.

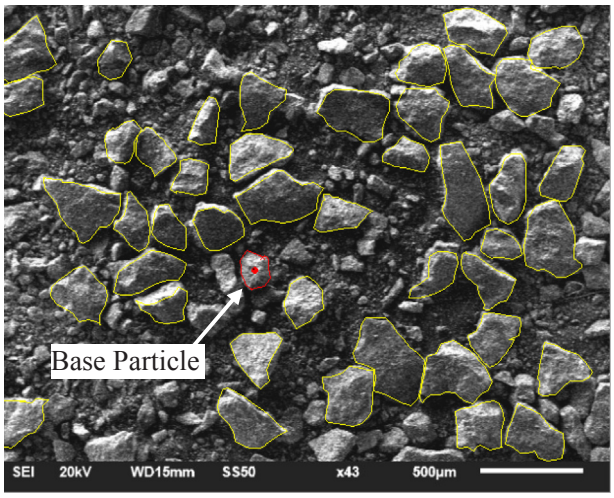

Fig. 3. Large particle count in the SEM image (VBTO-2) – The base particle is indicated by the arrow.

in both VG or VB foulants on tube surfaces made of Cr-Mo alloy.

These observations are in line with the findings of several laboratory studies made on petroleum corrosion as summarized in Table 4. At temperatures below 350 °C on carbon steel, corrosion is the predominant mechanism, as opposed to coke fouling [14,15]. This agrees with the identification of more than 50 wt% Fe plus S elements in the foulant samples studied here, which were deposited below 300 °C. Hence, Naphthenic acids (NAP, RCOOH) and sulphur compounds should be investigated as the main causing species. Also, as far as foulant thickness and corrosion rate of the surfaces made by Cr steel and CS alloy are concerned, similar observations to Refs. [16,17] were made in this study, indicating that less corrosion and more fouling may be expected with Cr alloy surfaces in comparable conditions. Additionally, the identification of Fe and O compositions in the foulant samples deposited on Cr steel alloy at higher temperatures reported in this work, as well as those investigated in Refs. [18–20] (see Table 4), indicate that deposition temperature also plays an important role on the corrosion reaction types involved and their resulting products. When faced with oxygen detection in examining corrosion products, its presence was previously dismissed in several laboratory studies as due to either exposure to air contamination or experimental errors [19].

Having reviewed the above evidence, a novel corrosion mechanism is proposed here to describe the fouling process experienced in the refinery exchangers where our foulant samples were collected. The presence of Cr in the alloys could enhance surface resistance against sulphur compounds attacks. However, at high temperatures (270–280 °C), the Cr alloy surface might not resist against NAP attacks, leading to Reaction (1) and production of oil-soluble iron naphthenates, (RCOO)2Fe, which have a size twice that of naphthenic acid. Hence, the larger (RCOO)2Fe would diffuse back to the bulk fluid more slowly than the NAP (responsible for acid attacks) diffuse from the bulk fluid to the tube surface, thereby, providing a diffusion barrier to the steel surface.

$$Fe + 2RCOOH \leftrightarrows (RCOO)2Fe + H_2 \quad (1)$$

On the other hand, as a result of an iron naphthenates possible reaction with H_2S (Reaction 2), FeS particulates may deposit on the barrier and, given time at this high temperature, the naphthenates decompose to FeO (Reaction 3). The latter is thermodynamically unstable, and hence disproportionates further to magnetite (Fe_3O_4) (Reaction 4). These seemingly stagnant compounds on the exchanger tube surfaces where heavy oil fractions such as VGO or VB are flowing, may transform into thick foulant layers. This would therefore justify the presence of thicker foulant layers and less corrosion observed at the hotter exchangers whose tube surfaces were made from Cr steel alloys, i.e. E3AB and E5 (see Table 1). Temperature in the downstream exchangers (E2AB, E1A and E4) was not high enough for Reaction 1 to take place, but as their surfaces were made from CS, sulphidation (Reaction 5) might have occurred, leading to the production of a FeS layer.

$$H_2S + (RCOO)2Fe \leftrightarrows FeS + 2RCOOH \quad (2)$$

$$(RCOO)2Fe \leftrightarrows FeO + CO_2 + RCOR \quad (3)$$

$$4FeO \leftrightarrows Fe_3O_4 + \alpha\text{-}Fe \quad (4)$$

$$Fe + H_2S \leftrightarrows FeS + H_2 \quad (5)$$

Although the produced FeS layer could protect the metal surface against subsequent H_2S attacks, it may be assumed that in this temperature range NAP reacts backward with FeS (Reaction 2) to stabilize the equilibrium by regenerating H_2S. FeS dissolution or delamination of primarily formed scales would encourage further sulphidation leading to more corrosion and less fouling, as experienced in the downstream exchangers named above.

As regards the presence of FeO(OH) in foulant samples from E3AB and E5, it is worth noting that no Fe_3O_4 (produced by Reaction 4) was identified in our XRD results. Fe_3O_4 might somehow have reacted with water and turned into FeO(OH) according to Reaction 6. Considering the unlikely presence of water in heavy oil fractions, water circulation

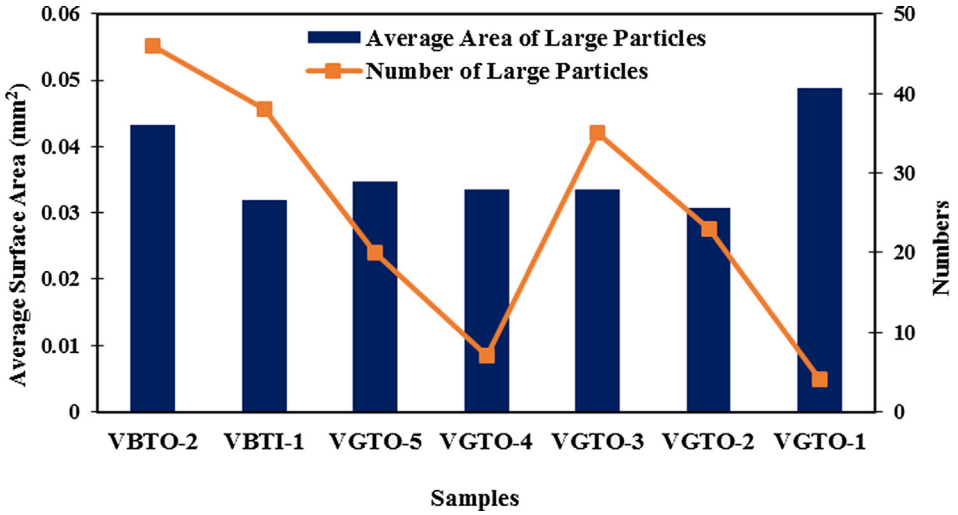

Fig. 4. Number of large particles and their average surface areas in the foulant samples.

Table 2
Fractions contents (wt%) specified with solvent extraction of raw foulant samples.

Samples	VGTO-1	VGTO-2	VGTO-3	VGTO-4	VGTO-5	VBTO-1	VBTI-2
Maltenes	24.76	19.74	18.18	17.98	15.86	14.56	7.35
Asphaltenes	–	–	–	–	–	2.47	3.21
Insoluble	75.24	80.26	81.82	82.02	84.14	82.96	89.44

and steam purging, carried out as a mandatory operation before dismantling the exchangers in a major shutdown, may have been responsible for such reaction and justify our results.

$$Fe_3O_4 + H_2O \leftrightarrows 2FeO(OH) \quad (6)$$

It should be noted that more Fe was observed in VBTI-2 sample collected from inside the Cr-Mo alloy tubes of E5 compared to the VBTO-1 sample from the CS outsides tube of E4. This could be explained by deposition of particulates originated from upstream equipment corrosion products or Fe compounds suspended in the fluid, for which it is required to examine the suspended solid particles content of VB at the entrance of the corresponding exchangers. This could also be carried out for VGO to determine the possible contribution of particulate deposition on forming thick fouling layers (1mm and above). It is postulated that the suspended particles might be dragged along with the heavy fractions streams and eventually settle in the product side of the heat exchangers. The attachment of such particles would indeed be facilitated by the presence of a deposit layer formed, initially, following a local corrosion mechanism as proposed above. At the high temperatures of the VGO and VB streams, the corrosion particles (e.g. FeS) may act as "nucleation" points for the formation of coke, which in turn could act as a gluing agent and lead to particle agglomeration [16]. From the time the particles detach at upstream equipment to the time when they deposit at the heat exchanger, the dimensions and characteristics of the particles would therefore evolve. This might explain the wide range of particle sizes observed in this study, as well as the differences between deposits formed by each fluid (VB and VGO) and at different locations along the line for each of them.

Additionally, to make the mechanism proposed here quantitative, determination of many parameters are required or alternatively simplifications may have to be made. A deposit generating rig (e.g. [21]) could be employed in future works to investigate how fouling and/or corrosion rate/s could be influenced by temperature and tube material. Deposition kinetics developed in controlled experiments could then be coupled with models that describe the deposit as a multi-component system undergoing chemical reactions [22]. This could be useful to account for the various deposition mechanisms and fouling species involved and, ultimately, evaluate how the thermo-hydraulic performance of the heat exchangers is affected by the growth of such heterogeneous deposits [23].

3.4. The existence of sulphur crystals

As can be seen in Fig. 5, a special peak is observed in the XRD patterns of VGTO-5 and 4 corresponding to sulphur (indexed by letter c). During the extraction analysis, after drying the *n*-heptane solvent by nitrogen flow, some crystals became evident in the maltenes jars of these samples as well as those of VGTO-3 (Fig. 6). Both sulphur allotropes illustrated in Fig. 7 [24] were seen in the VGTO-5 jar: two large orthorhombic crystals (2–4 mm in size) at the bottom, and a mass of monoclinic ones on the peripheral surface. For VGTO-4 and VGTO-3, only monoclinic crystals in larger sizes were observed. However, S crystal peaks were not identified in the XRD pattern of VGTO-3, perhaps due to smaller amount of S crystals being washed away by *n*-heptane during sample preparation of XRD examination. The tube material (CS) might also have played a role here through a sulphidation reaction.

4. Conclusions

A comprehensive investigation was carried out on the morphological, physical and chemical characteristics of seven foulant samples deposited below 300 °C by VGO and VB as heating fluids in preheaters of a constant feedstock distillation unit. Results show that more than 75 wt% of all samples were inorganics (indicated by insolubility in *n*-heptane and toluene), with 50 wt% FeS. Additionally, FeO(OH) was also deposited on hotter tube surfaces made from Cr steel alloy, where more fouling and less corrosion were evident. Our results are consistent with several recent petroleum corrosion laboratory studies. The role of temperature and tube material were reviewed and a mechanism was proposed to explain the corrosion fouling progress experienced. According to this model, at the temperature range of 270–300 °C, naphthenic acid attacks tube surfaces made from Cr steel alloy, leading to the formation of a corrosion-protective foulant layer consisting of FeO(OH) as well as FeS particulates, produced by reaction of H_2S and (RCOO)2Fe (iron naphthenates). For CS-tube exchangers working at lower temperatures, sulphidation creates FeS layers which delaminate

Table 3
Elements' contents (%wt) and crystalline compounds of foulant samples.

Samples	VGTO-1	VGTO-2	VGTO-3	VGTO-4	VGTO-5	VBTO-1	VBTI-2
C	3.99	1.61	1.81	2.22	2.08	4.23	3.27
H	0.99	0.97	0.91	1.37	1.60	1.27	1.35
N	0.24	0.85	1.64	1.60	2.61	3.28	1.63
O	17.08	19.02	17.92	33.49	39.24	43.95	39.17
S	25.70	26.11	25.70	21.54	19.42	14.40	13.39
Fe	51.10	50.58	50.61	39.02	34.53	29.10	39.61
Na	0.00	0.01	0.23	0.00	0.00	2.07	0.87
Mg	0.00	0.13	0.14	0.11	0.00	0.10	0.10
Ca	0.25	0.25	0.28	0.25	0.23	0.21	0.12
Si	0.27	0.04	0.19	0.14	0.13	0.44	0.26
Cl	0.03	0.10	0.03	0.00	0.00	0.74	0.09
V	0.04	0.02	0.08	0.26	0.14	0.14	0.13
Ni	0.32	0.31	0.45	0.01	0.00	0.07	0.01
Crystalline Compounds	FeS	FeS	FeS	FeS FeO(OH) S	FeO(OH) FeS S	FeS	FeS FeO(OH)

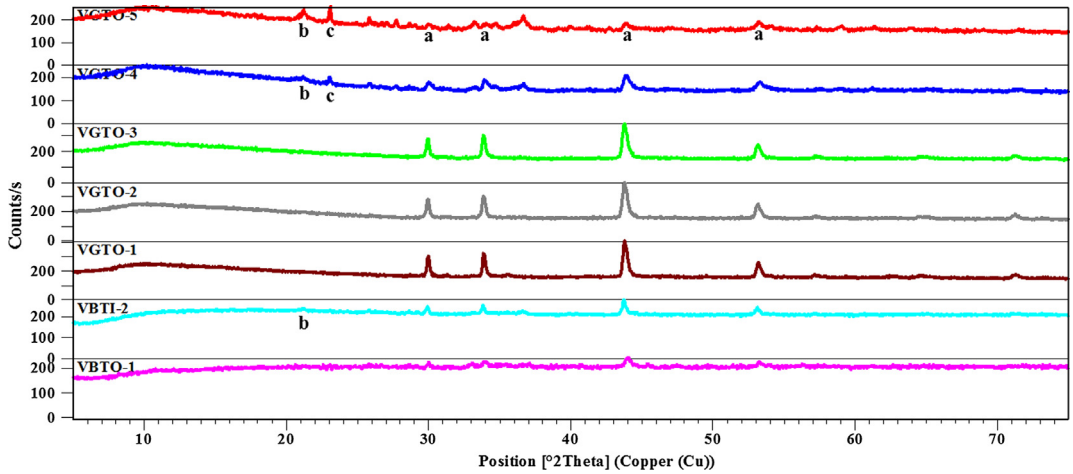

Fig. 5. Indexed XRD patterns of foulant samples (a, b and c stands respectively, for FeS, FeO(OH) and S).

Table 4
A summary of results for the latest laboratory case studies on petroleum corrosion.

No	Subject (Process fluid)	i) Observation/ii) Comment	Refs.
1	Iron sulphide and coke fouling (sour oil)	i) Prevalence of corrosion over coke fouling at temp < 350 °C ii) NAP and S compounds are main species, causing petroleum corrosion leading to FeS particulates or film fouling	[15]
2	Sulphide promoted chronic fouling on heat transfer surfaces made of different metallurgies at T_{bulk} = 290 °C, $T_{surface}$ = 490 °C (two crude oil blends)	i) Thicker foulant (~2×) on wire surface made of 9Cr-Mo steel compared to CS with the most cross section reduction ii) 'self-cleaning' behaviour of CS, i.e. sulphide forms on surface, but continuously delaminates during test, leading to reduced sulphide/coke build-up rates and its cross section	[16]
3	Competitive corrosion mechanisms of NAP and sulphur compounds (crude oil)	i) Corrosion layers formed on 5Cr steel surfaces were more protective against NAP attacks than those formed on CS surfaces	[17]
4	FeS protectiveness, NAP challenge attacks on FeS scale (VGO)	i) Presence of an iron oxide layer on the least corroded metal surface ii) A probable oxygen source of the oxide layer is NAP acids in the crude fraction, thermally decomposed during the test	[18]
5	Analysis of corrosion scales formed on CS and 5Cr steel surfaces in	i) The oxide layer (magnetite, Fe_3O_4) protected surface against NAP attacks, and not the	[19]
6	hydrocarbons containing different values of NAP and S compounds (crude oil)	FeS layer ii) Magnetite originated from NAP corrosion, iron naphthenates decomposition and disproportionation of FeO. – layers formed on 5Cr steel surfaces were more protective than those on CS surfaces, perhaps Cr acts as catalyst in forming magnetite and enhancing protectiveness – - No oxide scale, even in the presence of NAP, following similar experiments with first phase of scale formation at low temperature (232 °C), could prove the importance of higher temperatures in overcoming NAP corrosion compared to sulphidation	[20]

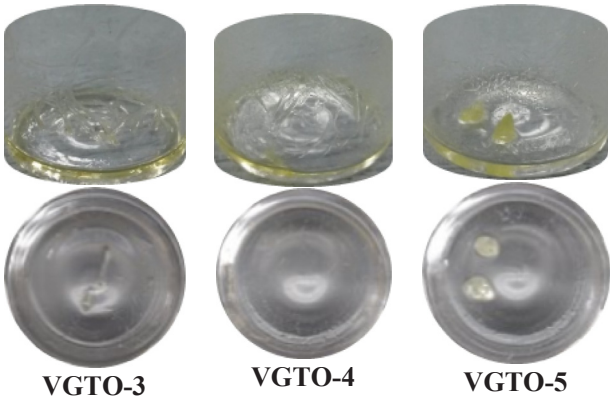

Fig. 6. Maltenes jars of VGTO-3, 4 and 5 samples, following drying with nitrogen flow. Sulphur crystals are clearly evident in both allotropes.

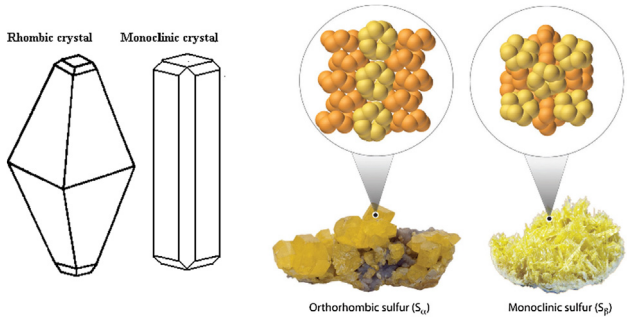

Fig. 7. Illustration of two allotropes of Sulphur [24].

by reacting with naphthenic acid, regenerating H_2S and causing further corrosion. This corrosion process could also explain the formation and detachment of particles in upstream equipment. After being dragged by the heavy fractions streams, and agglomerated over time into different sizes and morphologies, these particles might have deposit on the product side of the preheaters, leading to the observed deposit layers of 1 mm thickness and above.

The results not only agree with observations made in laboratory test, but also highlight the importance of studying deposits formed under industrial conditions, timescales and variation of the deposition

process, evidenced by the deposit characteristics, along extensive heat exchanger networks. Furthermore, XRD patterns indicated the existence of sulphur crystals in several of the VGO foulant samples, confirmed by observation in the forms of both allotropes in their maltenes fractions.

Acknowledgements

EB and MRM gratefully acknowledge collaboration of EORC refinery. Also, the authors wish to thank Dr Marcos Millan-Agorio for provision of laboratory facilities.

References

[1] Macchietto S, Hewitt GF, Coletti F, Crittenden BD, Dugwell DR, Galindo A, et al. Fouling in crude oil preheat trains: a systematic solution to an old problem. Heat Transf Eng 2011;32:197–215.
[2] Coletti F, Joshi HM, Macchietto S, Hewitt GF. Introduction to crude oil fouling. In: Coletti F, Hewitt GF, editors. Crude oil fouling depos. charact. meas. model. Boston: Gulf Professional Publishing; 2014.
[3] Crittenden BD, Kolaczkowski ST, Downey IL. Fouling of crude oil preheat exchangers. Trans IChemE Part A Chem Eng Res Des 1992;70:547–57.
[4] Brons G, Brown LD, Joshi HM, Kennedy RJ, Bruno T, Rudy TM. Method for refinery foulant deposit characterization. US 2006/0014296Al; 2006.
[5] Bennett CA, Appleyard S, Gough M, Hohmann RP, Joshi HM, King DC, et al. Industry-recommended procedures for experimental crude oil preheat fouling research. Heat Transf Eng 2006;27:28–35. http://dx.doi.org/10.1080/01457630600845788.
[6] Venditti S, Berrueco C, Alvarez P, Morgan TJ, Millan M, Herod AA, et al. Developing characterisation methods for foulants deposited in refinery heat exchangers. In Int. conf. heat exch. fouling clean. VIII, vol. 2009, Schladming, Austria; 2009. p. 44–51.
[7] Young A, Venditti S, Berrueco C, Yang M, Waters A, Davies H, et al. Characterization of crude oils and their fouling deposits using a batch stirred cell system. Heat Transf Eng 2011;32:216–27. http://dx.doi.org/10.1080/01457632.2010.495603.
[8] Chew J, Joshi HM, Kazarian SG, Millan-Agorio M, Tay FH, Venditti S. Deposit characterization and measurements. In: Coletti F, Hewitt GF, editors. Crude oil fouling, first Elsevier Inc.; 2015. p. 95–178. http://dx.doi.org/10.1016/B978-0-12-801256-7.00004-X.
[9] Mozdianfard MR, Behranvand E. A field study of fouling in CDU preheaters at Esfahan refinery. Appl Therm Eng 2013;50:908–17. http://dx.doi.org/10.1016/j.applthermaleng.2012.08.025.
[10] Mozdianfard MR, Behranvand E. Fouling at post desalter and pre flash drum heat exchangers of CDU preheat train. Appl Therm Eng 2015;89:783–94. http://dx.doi.org/10.1016/j.applthermaleng.2015.06.045.
[11] Brons G, Brown LD, Joshi HM, Kennedy RJ, Bruno T, Rudy TM. Method for refinery foulant deposit characterization. US 2006/0014296 Al; 2010.
[12] Puron H, Pinilla JL, Berrueco C, la Fuente JAMD, Millan M. Hydrocracking of maya vacuum residue with NiMo catalysts supported on mesoporous alumina and silica–alumina. Energy Fuels 2013;27:3952–60.
[13] Puron H, Chin KK, Pinilla JL, Fidalgo B, Millan M. Kinetic analysis of vacuum residue hydrocracking in early reaction stages. Fuel 2014;117:408–14. http://dx.doi.org/10.1016/j.fuel.2013.09.053.
[14] Srinivasan M, Watkinson AP. Fouling of some Canadian crude oils. Heat Transf Eng 2005;26:7–14. http://dx.doi.org/10.1080/01457630590889988.
[15] Wang W, Watkinson AP. Iron sulphide and coke fouling from sour oils: review and initial experiments. Int conf heat exch. fouling clean, vol. 2011. 2011. p. 23–30.
[16] Hazelton M, Stephenson T, Lepore J, Subramani V, Mitlin D. Sulfide promoted chronic fouling in a refinery: a broad phenomenon spanning a range of heat transfer surfaces and oil types. Fuel 2015;160:479–89. http://dx.doi.org/10.1016/j.fuel.2015.07.074.
[17] Bota G, Nesic S. Naphthenic acid challenges to iron sulfide scales generated in-situ from model oils on mild steel at high temperature. NACE int corros conf expo. 2013. p. 1–13.
[18] Bota GM, Farelas F, Robbins W, Nesic S. Evaluation of scales protective properties in naphthenic acid challenges. 248th ACS Natl Meet Expo. 2014. p. 546.
[19] Jin P, Nesic S, Wolf HA. Analysis of corrosion scales formed on steel at high temperatures in hydrocarbons containing model naphthenic acids and sulfur compounds. Surf Interface Anal 2015;47:454–65. http://dx.doi.org/10.1002/sia.5733.
[20] Jin P, Bota G, Robbins W, Nesic S. Analysis of oxide scales formed in the naphthenic acid corrosion of carbon steel. Energy Fuels 2016. http://dx.doi.org/10.1021/acs.energyfuels.6b01066.
[21] Tajudin Z, Martinez-Minuesa JA, Diaz-bejarano E, Valkov I, Orzlowski P, Coletti F, et al. Experiment analysis and baseline hydraulic characterisation of HiPOR, a high pressure crude oil fouling rig. Chem Eng Trans 2015;43:1405–10. http://dx.doi.org/10.3303/CET1543235.
[22] Diaz-bejarano E, Coletti F, Macchietto S. Impact of complex layering structures of organic and inorganic foulants on the thermo-hydraulic performance of a single heat exchanger tube – a simulation study. Ind Eng Chem Res 2016;55:10718–34. http://dx.doi.org/10.1021/acs.iecr.6b02330.
[23] Diaz-bejarano E, Behranvand E, Coletti F, Mozdianfard MR, Macchietto S. Organic and inorganic fouling in heat exchangers – industrial case study: analysis of fouling state. Appl Energy 2017;206:1250–66.
[24] Chemistry of sulfur. UC Davis ChemWiki n.d. < http://chemwiki.ucdavis.edu/Core/Inorganic_Chemistry/Descriptive_Chemistry/Elements_Organized_by_Block/2_p-Block_Elements/Group_16:_The_Oxygen_Family/Chemistry_of_Sulfur > , 2016.